ACS OMEGA

Open Access

http://pubs.acs.org/journal/acsodf

Article

Effect of Position of Donor Units and Alkyl Groups on Dye-Sensitized Solar Cell Device Performance: Indoline−Aniline Donor-Based Visible Light Active Unsymmetrical Squaraine Dyes

Amrita Singh, Ambarish Kumar Singh, Ruchi Dixit, Kumar Vanka, Kothandam Krishnamoorthy,* and Jayaraj Nithyanandhan*

Cite This: *ACS Omega* 2024, 9, 16429−16442

Read Online

ACCESS | Metrics & More | Article Recommendations | Supporting Information

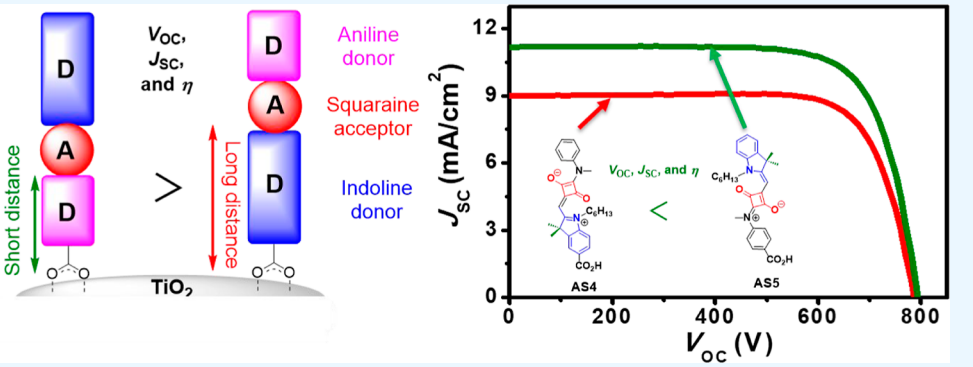

ABSTRACT: Indoline (In) and aniline (An) donor-based visible light active unsymmetrical squaraine (SQ) dyes were synthesized for dye-sensitized solar cells (DSSCs), where the position of An and In units was changed with respect to the anchoring group (carboxylic acid) to have In-SQ-An-CO_2H and An-SQ-In-CO_2H sensitizers, **AS1**−**AS5**. Linear or branched alkyl groups were functionalized with the N atom of either In or An units to control the aggregation of the dyes on TiO_2. **AS1**−**AS5** exhibit an isomeric π-framework where the squaric acid unit is placed in the middle, where **AS2** and **AS5** dyes possess the anchoring group connected with the An donor, and **AS1**, **AS3**, and **AS4** dyes having the anchoring group connected with the In donor. Hence, the conjugation between the middle squaric acid acceptor unit and the anchoring $-CO_2H$ group is short for **AS2**, **AS5**, and **AK2** and longer for **AS1**, **AS3**, and **AS4** dyes. **AS** dyes showed absorption between 501 and 535 nm with extinction coefficients of 1.46−1.61 × 10^5 M^{-1} cm^{-1}. Further, the isomeric π-framework of An-SQ-In-CO_2H and In-SQ-An-CO_2H exhibited by means of changing the position of In and An units a bathochromic shift in the absorption properties of **AS2** and **AS5** compared to the **AS1**, **AS3**, and **AS4** dyes. The DSSC device fabricated with the dyes contains short acceptor-anchoring group distance (**AS2** and **AS5**) showed high photovoltaic performances compared to the dyes having longer distance (**AS1**, **AS3**, and **AS4**) with the iodolyte (I^-/I_3^-) electrolyte. DSSC device efficiencies of 5.49, 6.34, 6.16, and 5.57% have been achieved for **AS1**, **AS2**, **AS3**, and **AS4** dyes, respectively; without chenodeoxycholic acid (CDCA), small changes have been observed in the device performance of the **AS** dyes with CDCA. Significant changes have been noted in the DSSC parameters (open-circuit voltage V_{OC}, short-circuit current J_{SC}, fill factor ff, and efficiency η) for the **AS5** dye while sensitized with CDCA and showed highest DSSC efficiency of 8.01% in the **AS** dye series. This study revealed the potential of shorter SQ acceptor-anchoring group distance over the longer one and the importance of alkyl groups on the overall DSSC device performance for the unsymmetrical squaraine dyes.

1. INTRODUCTION

Dye-sensitized solar cells (DSSCs) have been considered as an alternative source of clean energy for the future due to their advantages over the first- and second-generation solar cells in terms of production costs, weight, flexibility, scalability, and works in diffused or reflected light conditions.[1−8] The operational performance under artificial light conditions with the high device efficiency output makes DSSCs a potential and promising technology for harvesting indoor lights over the silicon solar cells.[9−12] A multidisciplinary and concerted research has been performed over the last two decades for commercializing DSSC devices. The dye anchored on the

Received: January 4, 2024
Revised: March 8, 2024
Accepted: March 11, 2024
Published: March 26, 2024

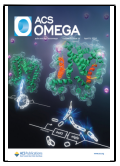

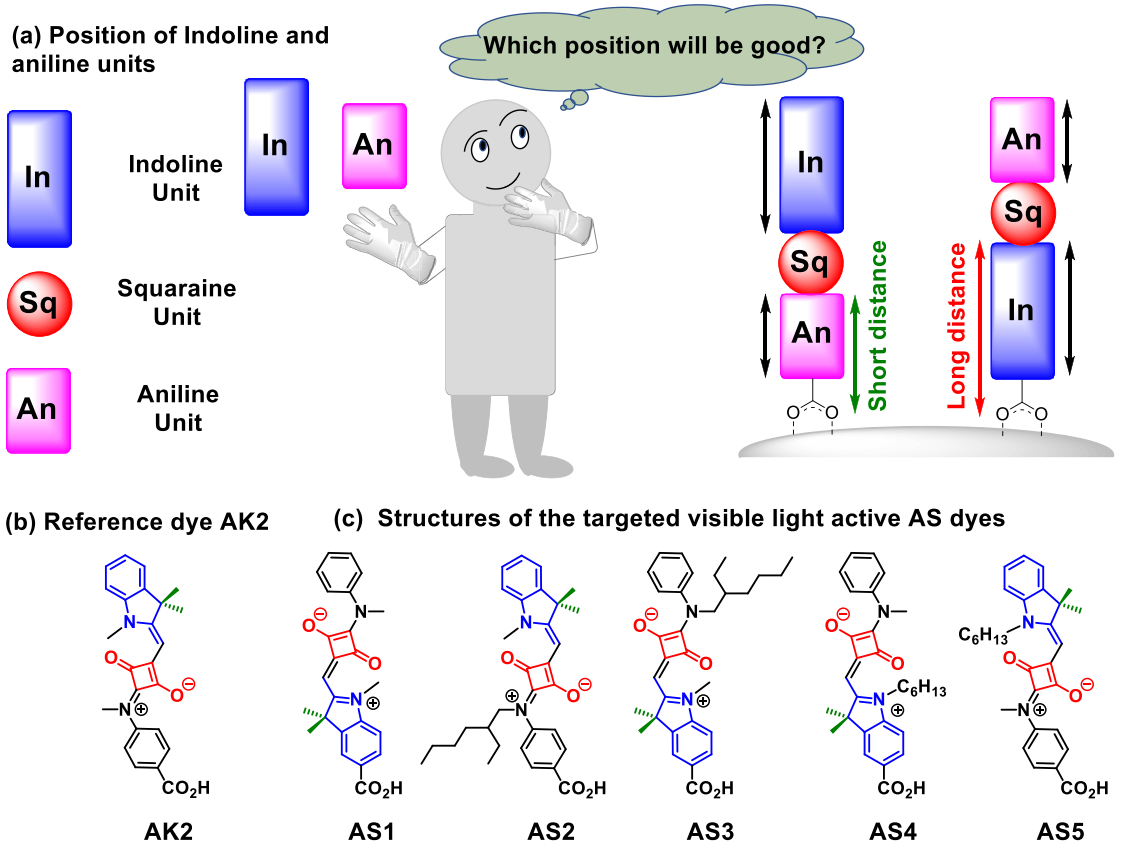

Figure 1. (a) Dye design with variations in the position of In and An units in visible light active unsymmetrical squaraine dyes and (b) structures of visible light active **AK2** (reference dye) and targeted **AS1−5** dyes.

mesoporous TiO_2 surface is the main component which determines the overall device performance and stability;[13] therefore, designing new sensitizers that can efficiently absorb solar light from the various solar regions and convert it into electricity is one of the major research topics in DSSCs.[4,14] Since 1991, transition metal-containing dyes (ruthenium complexes) and organic dyes are commonly used sensitizers in DSSCs.[15,16] Structurally engineered sensitizers with electronic and steric effects achieved a DSSC device efficiency of 13.0% for the porphyrin dye[17] and 11.7% for the ruthenium dye.[18] The metal-free organic dye has achieved an efficiency of 13.6%,[19] and cosensitizing with optically complementary dyes helped to enhance the performance to 15.2%.[20] A DSSC device performance of 37%[21] has been achieved under the dim light condition (6000 l×) and 10.0% for DSSC-based small modules.[22,23] Among them, organic sensitizers have attracted great attention of researchers due to diversity in the tuning of donor, acceptor, and π-spacer moieties that absorb solar light from visible to near-infrared regions.[24,25] Organic sensitizers with the dye architectures of donor−acceptor (D−A), donor−π−acceptor (D−π−A), donor−acceptor−π−acceptor (D−A−π−A), and donor−donor−π−acceptor (D−D−π−A) for harvesting most of the solar light have been employed. Further, the effect of the position of donor, acceptor, and π-spacer moieties has been studied in DSSCs.[24−29] Further, charge injection and dye regeneration processes of a DSSC device are strongly affected by the distance and interactions between the anchoring group and the acceptor unit of the dyes.[30−33] The alkyl group-wrapped far-red and visible light active unsymmetrical squaraine dyes have been explored for DSSCs.[34−38] Squaraine dyes belong to the family of polymethine chromophores and exhibit a sharp transition with high extinction coefficient (>10^5 M^{-1} cm^{-1}) in the far-red region of the solar spectrum and also form well-defined H- and J-aggregated structures both in solution and on the metal oxide surface.[39,40] The self-assembled structures of the squaraine dyes have the variety of applications, such as in organic photovoltaic, sensors, and DSSCs.[41,42] In our previous work, we have systematically studied the effect of alkyl-group-wrapping, position of anchoring group, best sensitizing solvents/electrolytes, and effect of changing the donor moieties for unsymmetrical squaraine on the DSSC performance.[35−37,43−48] Recently, it has been reported that aniline (An) and indoline (In) donors containing unsymmetrical squaraine dyes absorb in the visible region centered at 520 nm with an extinction coefficient of >10^5 M^{-1} cm^{-1}. Furthermore, the alkyl group-wrapped visible light active squaraine dye, **AK4** (η = 7.73%), and the dye with methyl groups, **AK2** (η = 7.34%), showed good device performance,[35] and the effect of position of donor units within the squaraine dye framework has not been studied. In this study, the structures of In and An donor-based unsymmetrical squaraine dyes have been modulated by keeping the shorter An and slightly longer In donors between the acceptor and anchoring units to evaluate their effect on DSSC device performance. A series of visible light-responsive squaraine **AS** dyes with changes in the position of donor units (where small linear and branched alkyl groups were placed systematically at the N atoms of An and In donors) have been designed and synthesized for DSSCs. Further, the importance of the effect of the position of alkyl groups also included in the present set of **AS** dyes (Figure 1).

https://doi.org/10.1021/acsomega.4c00123
ACS Omega 2024, 9, 16429−16442

2. EXPERIMENTAL SECTION

Compounds **1**,[35] **2**,[43] **3**,[54] **4**,[44] and **11**[36] were synthesized using the procedure provided in the literature. 3,4-Dibutoxycyclobut-3-ene-1,2-dione (**5**), An (**8**), 4-aminobenzoic acid (**9**), *N*-methylaniline (**12**), and 4-(methylamino)benzoic acid (**13**) were procured from the commercial sources.

2.1. General Methods and Instrumentation. General methods for synthesizing the targeted dyes, techniques utilized for structural characterization of newly synthesized AS dyes, and methods used for photophysical and electrochemical properties of the sensitizers are provided in the Supporting Information.

2.2. Synthesis of AS Dyes. *2.2.1. 2-((2-Butoxy-3,4-dioxocyclobut-1-en-1-yl)methylene)-1-hexyl-3,3-dimethylindoline-5-carboxylic Acid (**6**).* Compound **4** (0.9 g, 2.16 mmol) and 3,4-dibutoxycyclobut-3-ene-1,2-dione (**5**) (0.49 g, 2.16 mmol) were dissolved in 20 mL of *n*-BuOH in a round-bottom flask (100 mL), triethylamine (0.55 g, 5.4 mmol) was added, stirred at room temperature for 12 h, and then the reaction mixture was heated for 2 h at 70 °C. The reaction mixture was cooled to room temperature, and solvents were removed under reduced pressure and purified with column chromatography (SiO_2, 100−200 mesh) with using MeOH and CH_2Cl_2. Yield: 500 mg, 52%. ^{1}H NMR (400 MHz, $CDCl_3$): δ 8.09 (dd, J = 8.38, 1.63 Hz, 1H), 7.98 (d, J = 2 Hz, 1H), 6.90 (d, J = 8 Hz, 1H), 5.51 (s, 1H), 4.88 (t, J = 6.63 Hz, 2H), 3.84 (t, J = 7.50 Hz, 2H), 1.83−1.95 (m, 2H), 1.76 (t, J = 7.00 Hz, 2H), 1.49−1.58 (m, 2H), 1.31−1.47 (m, 6H), 1.02 (t, J = 7.44 Hz, 3H), 0.87−0.95 (m, 3H). ^{13}C NMR (101 MHz, $CDCl_3$): δ ppm 13.6, 13.9, 18.7, 22.4, 26.2, 26.6, 27.0, 31.3, 32.1, 43.1, 47.3, 74.1, 83.2, 107.7, 122.9, 123.87, 131.5, 140.8, 147.5, 167.3, 171.1, 173.4, 188.5, 188.8, 192.3.

*2.2.2. 2-((2-Butoxy-3,4-dioxocyclobut-1-en-1-yl)-methylene)-1-hexyl-3,3-dimethylindoline-5-carboxylic Acid (**7**).* Compound **6** (0.45 g, 1.02 mmol) was dissolved in 10 mL of acetone, and 2 N aqueous HCl (3 mL) was added to the above mixture and refluxed for 12 h. The reaction mixture was cooled to room temperature, and solvents were removed under reduced pressure and dried. Yield: 0.25 g, 55%. ^{1}H NMR (400 MHz, DMSO-d_6): δ 7.88 (s, 1H), 7.86 (d, J = 4 Hz, 1H), 7.14 (d, J = 8.39 Hz, 1H), 5.59 (s, 1H), 3.87 (t, J = 7.25 Hz, 2H), 1.59−1.67 (m, 2H), 1.56 (s, 6H), 1.24−1.39 (m, 6H), 0.83 (t, J = 7.25 Hz, 3H). ^{13}C NMR (101 MHz, DMSO-d_6): 14.2, 22.4, 26.2, 26.2, 27.2, 31.3, 46.8, 83.7, 108.4, 123.3, 124, 130.8, 140.5, 147.3, 164.8, 167.7, 174.5, 193.

*2.2.3. N-(2-Ethylhexyl)aniline (**10**).* An (**8**) (0.7 g, 7.51 mmol) and 2-ethylhexanal (1.15 g, 9.01 mmol) were dissolved in 20 mL of anhydrous CH_2Cl_2, 1 mL of acetic acid was added in a 100 mL round-bottom flask and stirred at rt for 1 h, and then $NaBH(OAc)_3$ (3.18 g, 15.03 mmol) was added in a reaction flask and stirred at room temperature for 12 h; after that, the reaction mixture was quenched with $NaHCO_3$ aqueous solution, the organic layer was extracted with CH_2Cl_2 (3 × 30 mL), dried over Na_2SO_4, concentrated, and purified with 97.5% pet ether and 2.5% EtOAc. Yield: 0.85 g, 55%. ^{1}H NMR (500 MHz, DMSO-d_6): δ 7.00−7.07 (m, 2H), 6.52−6.57 (m, 2H), 6.44−6.50 (m, 1H), 5.46 (t, J = 5.63 Hz, 1H), 2.88 (t, J = 6.07 Hz, 2H), 1.47−1.58 (m, 1H), 1.29−1.41 (m, 4H), 1.24−1.28 (m, 4H), 0.79−0.93 (m, 6H). ^{13}C NMR (125 MHz, $CDCl_3$): 15.9, 19.2, 27.8, 29.0, 33.6, 35.8, 43.2, 51.3, 116.9, 120.3, 134.0, 154.4. General procedure for the synthesis of AS dyes: semisquaric acid derivative (1 equiv) and corresponding An derivative (1 equiv) were dissolved in anhydrous toluene and *n*-BuOH (1:1, 10 mL of each) in a 50 mL round-bottomed flask and charged with the Dean−Stark distillation apparatus. The reaction mixture was refluxed for 16 h under an inert atmosphere. After completion of the reaction, solvents were removed and purified by column chromatography (SiO_2, 100−200 mesh, MeOH and CH_2Cl_2) to obtain the required dyes.

*2.2.4. 2-((-5-Carboxy-1,3,3-trimethylindolin-2-ylidene)-methyl)-4-(methyl(phenyl)iminio)-3-oxocyclobut-1-en-1-olate (**AS1**).* Compound **1** (0.2 g, 0.63 mmol) and *N*-methylaniline (**12**) (0.070 g, 0.63 mmol), orange solid, filtered and dried under reduced pressure. Yield: 150 mg, 56%. mp: 248 °C. ^{1}H NMR (400 MHz, $CDCl_3$): δ 8.09 (dd, J = 8.39, 1.53 Hz, 1H), 8.00 (d, J = 1.53 Hz, 1H), 7.41−7.54 (m, 4H), 7.31−7.41 (m, 1H), 6.96 (d, J = 8.39 Hz, 1H), 5.88 (s, 1H), 4.06 (s, 3H), 3.48 (s, 3H), 1.75 (s, 6H); ^{13}C NMR (101 MHz, $CDCl_3$): 27.4, 30.4, 39.3, 46.0, 48.0, 86.7, 107.9, 122.8, 123.8, 127.8, 129.0, 131.2, 140.3, 141.4, 147.4, 169.1, 170.6, 174.5, 180.2. IR (cm^{-1}): 3005, 2924, 2862, 1758, 1695, 1602, 1574, 1501, 1446, 1398, 1356, 1275, 1217, 1096, 1054, 926. HRMS (m/z): $[M]^+$ calcd for $C_{24}H_{22}O_4N_2$, 402.1580; found, $[M + H]^+$ 403.1653.

*2.2.5. 4-((4-Carboxyphenyl)(2-ethylhexyl)iminio)-3-oxo-2-((1,3,3-trimethylindolin-2-ylidene) methyl)cyclobut-1-en-1-olate (**AS2**).* Compound **2** (0.2 g, 0.74 mmol) and 4-((2-ethylhexyl)amino)benzoic acid (**11**) (0.18 g, 0.74 mmol), orange solid, filtered and dried. Yield: 230 mg, 60%. mp: 250 °C. ^{1}H NMR (400 MHz, $CDCl_3$): δ 8.06 (d, J = 8.63 Hz, 2H), 7.29−7.42 (m, 4H), 7.14 (t, J = 7.50 Hz, 1H), 7.00 (d, J = 7.88 Hz, 1H), 5.85 (br. s., 1H), 4.30−4.59 (m, 2H), 3.51 (br. s., 3H), 1.75 (br. s., 5H), 1.46−1.58 (m, 1H), 1.15−1.45 (m, 9H), 0.80−0.93 (m, 6H); ^{13}C NMR (101 MHz, $CDCl_3$): 10.5, 13.9, 22.8, 23.3, 27.2, 28.3, 29.8, 37.2, 48.9, 54.4, 85.5, 109.0, 122.1, 123.6, 124.0, 127.8, 129.4, 131.1, 142.0, 167.5, 171.2, 177.0, 180.6. IR (cm^{-1}): 2957, 2924, 2863, 1760, 1707, 1601, 1565, 1486, 1453, 1426, 1403, 1307, 1267, 1204, 1102, 1069, 1016, 982, 924. HRMS (m/z): $[M]^+$ calcd for $C_{31}H_{36}O_4N_2$, 500.2675; found, $[M + H]^+$ 501.2748.

*2.2.6. 2-((5-Carboxy-1,3,3-trimethylindolin-2-ylidene)-methyl)-4-((2-ethylhexyl)(phenyl)iminio)-3-oxocyclobut-1-en-1-olate (**AS3**).* Compound **1** (0.2 g, 0.63 mmol) and *N*-(2-ethylhexyl)aniline (**10**) (0.13 g, 0.63 mmol), orange color solid, filtered and dried under reduced pressure. Yield: 200 mg, 60%. mp: 210 °C. ^{1}H NMR (500 MHz, $CDCl_3$): δ 8.08 (dd, J = 8.20, 1.72 Hz, 1H), 7.98 (d, J = 1.53 Hz, 1H), 7.48 (t, J = 7.82 Hz, 2H), 7.32−7.43 (m, 3H), 6.93 (d, J = 8.39 Hz, 1H), 5.84 (s, 1H), 4.45−4.52 (m, 1H), 4.36−4.44 (m, 1H), 3.45 (s, 3H), 1.74 (s, 6H), 1.48−1.56 (m, 1H), 1.38−1.44 (m, 2H) 1.29−1.37 (m, 2H), 1.18−1.27 (m, 5H) 0.82−0.88 (m, 6H); ^{13}C NMR (126 MHz, $CDCl_3$): 10.4, 13.9, 22.8, 23.2, 27.5, 28.0, 28.3, 29.8, 30.2, 37.1, 47.8, 55.1, 86.6, 107.7, 123.6, 123.8, 124.4, 128.2, 129.0, 131.2, 137.9, 141.3, 147.5, 168.4, 170.7, 174.5, 176.7, 179.5, 182.3. IR (cm^{-1}): 2960, 2927, 2866, 1762, 1703, 1607, 1576, 1508, 1429, 1360, 1275, 1217, 1106, 1060, 937. HRMS (m/z): $[M]^+$ calcd for $C_{31}H_{36}O_4N_2$, 500.2675; found, $[M + H]^+$ 501.2748.

*2.2.7. 2-((-5-Carboxy-1-hexyl-3,3-dimethylindolin-2-ylidene)methyl)-4-(methyl(phenyl)iminio)-3-oxocyclobut-1-en-1-olate (**AS4**).* Compound **7** (0.2 g, 0.589 mmol) and *N*-methylaniline (**12**) (0.089 g, 0.589 mmol), orange color solid, filtered and dried under reduced pressure. Yield: 200 mg, 70%. mp: 180 °C. ^{1}H NMR (400 MHz, $CDCl_3$): δ 8.09 (d, J = 8.75 Hz, 2H), 7.45 (d, J = 8.88 Hz, 2H), 7.30−7.39 (m, 2H), 7.15−7.22 (m, 1H), 7.02 (d, J = 8.00 Hz, 1H), 5.95 (s, 1H), 4.03 (s, 3H), 3.93−4.02 (m, 2H), 1.77−1.87 (m, 2H), 1.76 (s, 6H),

https://doi.org/10.1021/acsomega.4c00123
ACS Omega 2024, 9, 16429−16442

Scheme 1. Synthesis of An and In Donor-Based Visible Light Active Squaraine Dyes (AS Dyes)

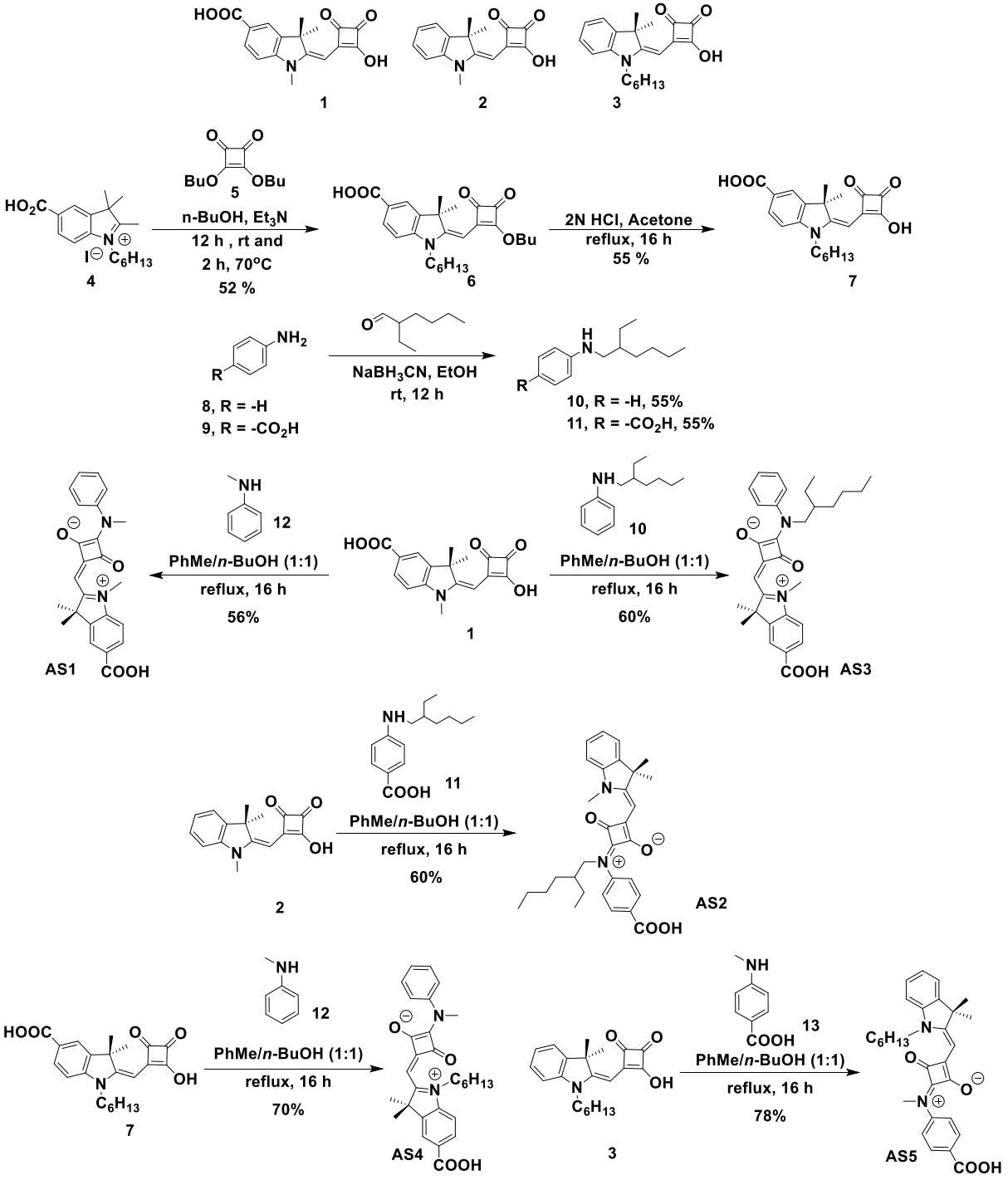

1.38−1.49 (m, 2H), 1.28−1.38 (m, 4H), 0.84−0.93 (m, 3H); ^{13}C NMR (101 MHz, $CDCl_3$): 13.9, 22.4, 26.6, 26.9, 27.1, 31.4, 43.7, 49.4, 85.8, 109.6, 121.8, 122.2, 124.1, 127.8, 127.8, 131.1, 142.0, 142.1, 144.5, 168.4, 171.6, 175.3, 181.8. IR (cm^{-1}): 2954, 2928, 2859, 1760, 1702, 1603, 1572, 1502, 1448, 1405, 1356, 1280, 1217, 1179, 1137, 1104, 1049, 934. HRMS (m/z): $[M]^+$ calcd for $C_{28}H_{32}O_4N_2$, 472.2360; found, $[M + H]^+$ 473.2435.

*2.2.8. 4-((4-Carboxyphenyl)(methyl)iminio)-2-((1-hexyl-3,3-dimethylindolin-2-ylidene)methyl)-3-oxocyclobut-1-en-1-olate (**AS5**).* Compound **3** (0.15 g, 0.39 mmol) and 4-(methylamino) benzoic acid (**13**) (0.042 g, 0.391 mmol), orange color solid, filtered and dried under reduced pressure. Yield: 150 mg, 78%. mp: 228 °C. ^{1}H NMR (400 MHz, $CDCl_3$): δ 8.09 (dd, J = 8.32, 1.69 Hz, 1H), 8.01 (d, J = 1.50 Hz, 1H), 7.41−7.51 (m, 4H), 7.33−7.39 (m, 1H), 6.95 (d, J = 8.38 Hz, 1H), 5.92 (s, 1H), 4.06 (s, 3H), 3.92 (t, J = 7.57 Hz, 2H), 1.81 (br. s., 2H), 1.75 (s, 6H), 1.36−1.46 (m, 2H), 1.21−1.34 (m, 4H), 0.87 (m, J = 7.06 Hz, 3H); ^{13}C NMR (101 MHz, $CDCl_3$): 13.9, 22.4, 26.6, 26.6 27.4, 31.4, 39.2, 43.4, 48.1, 86.6, 108.2, 122.8, 123.6, 123.9, 127.7, 129.1, 131.2, 140.3, 141.5, 147.1, 168.6, 170.7, 180.2, 180.7. IR (cm^{-1}): 3009, 2924, 2859, 1760, 1701, 1599, 1566, 1485, 1450, 1395, 1357, 1284, 1226, 1137, 1090, 923. HRMS (m/z): $[M]^+$ calcd for $C_{28}H_{32}O_4N_2$, 472.2360; found, $[M + H]^+$ 473.2435.

https://doi.org/10.1021/acsomega.4c00123
ACS Omega 2024, 9, 16429−16442

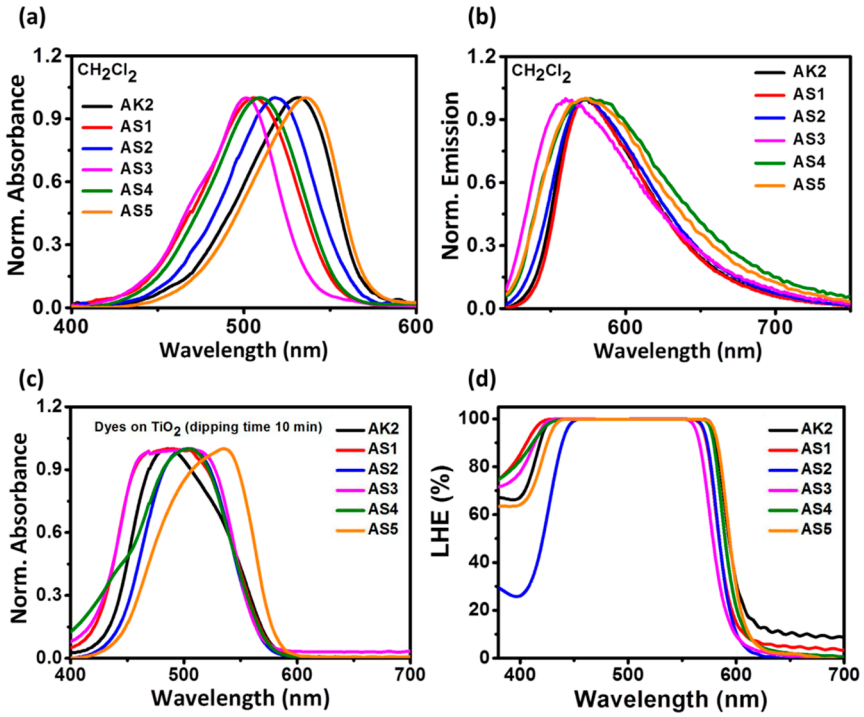

Figure 2. (a) Normalized UV−vis spectra of **AS** and **AK2** dyes in CH_2Cl_2 solution, (b) fluorescence spectra of **AS** and **AK2** dyes in CH_2Cl_2 solution, (c) normalized UV−vis spectra of **AS** and **AK2** dyes on TiO_2 (the thickness of the TiO_2 electrode was 6 μm, and the dipping time was 10 min), and (d) LHE (=1−10^{-A}) profiles of **AS** and **AK2** dyes on TiO_2 electrodes (thickness 6 μm and dipping time 12 h).

2.3. DSSC Fabrication. The procedure followed for the DSSC device fabrication and device characterization methods is provided in the Supporting Information.

3. RESULTS AND DISCUSSION

3.1. Synthesis of In−An Donor-Based AS Dyes. The synthesis of In-SQ-An-CO_2H- and An-SQ-In-CO_2H-based visible active unsymmetrical squaraine dyes with varied positions of donor units comprised a condensation reaction between the semisquaric acid derivatives and corresponding An derivatives. To obtain the required semisquaric acid derivatives, **1**, **2**, **3**, and **7**, we have followed the reported procedures which involve Fischer indole reaction for In synthesis, Fischer's base synthesis by the alkylation of In with alkyl iodide, formation of semisquaraines by treating Fischer's base with dibutoxysquarate, followed by deprotection transformation. *N*-Methylaniline (**12**), 4-amino-benzoic acid (**9**), and 4-*N*-methylamino-benzoic acid (**13**) are commercially available derivatives of An, whereas derivatives **10** and **11** were synthesized by condensation of corresponding amine with 2-ethylhexanal, followed by the reduction reaction with $NaBH_3CN$. Finally, semisquaric acid derivatives condensed with the An derivatives (1 equiv) in anhydrous toluene and *n*-BuOH (1:1) to obtain the required **AS** dyes (Scheme 1).

3.2. Photophysical and Electrochemical Properties. UV−vis measurements for the **AS1**−**AS5** dyes have been carried out in CH_2Cl_2 solution as well as on the TiO_2 surface (with a short dipping time of 10 min) to evaluate the absorbance properties of the dyes in solution and on the metal oxide surface. The UV−vis spectra for **AS** dyes along with reference dye **AK2** are provided in Figure 2 and Table 1. In CH_2Cl_2 solution, the absorbance maxima for the **AS** dyes have been found between 501 and 535 nm and showed its molar extinction coefficients between 1.46 and 1.61 × 10^5 M^{-1} cm^{-1} (Figure 2 and Table 1). Here, **AS** dyes with a shorter acceptor-anchoring group distance (In-SQ-An-CO_2H) showed a 12 nm blue shift for the **AS2** dye and a 5 nm red shift for the **AS5** dye, whereas **AS** dyes with a longer acceptor-anchoring group distance for **AS1**, **AS3**, and **AS4** (An-SQ-In-CO_2H) showed a 21−29 nm blue shift compared to reference dye **AK2** in CH_2Cl_2 solution. The obtained 25 nm blue shift for the **AS1** dye in CH_2Cl_2 solution is due to the change in the distance between the acceptor-anchoring group, whereas the 12 nm blue shift for the **AS2** dye and the 5 nm red shift for the **AS5** dye are due to the interactions between solvent and alkyl groups compared to reference dye **AK2**. Similarly, the obtained differences in the absorbance maxima for **AS3** and **AS4** dyes are due to the long acceptor-anchoring group distance and interactions between the solvent and alkyl groups compared to reference dye **AK2**. Further, **AS** dyes with 10 min sensitization time on the TiO_2 surface showed the absorbance maxima between 490 and 535 nm, where the **AS5** dyes showed the absorbance maxima like the solution, and **AS1** and **AS3** dyes showed broad absorbance compared to other **AS** dyes. Dyes belonging to the **AS** series showed the emission maxima between 560 and 572 nm with an onset of >700 nm. **AS** dyes with the small acceptor-anchoring group distance showed similar emission maxima (572 nm) like reference dye **AK2**, whereas dyes with longer acceptor-anchoring group distance showed different emission maxima. Dye anchoring on the TiO_2 surface has been characterized by IR spectroscopy, and the carbonyl stretching frequencies for the squaric acid and carboxylic acid units appeared at 1565, 1599, and 1709 cm^{-1}, respectively. Upon sensitizing with TiO_2, the carbonyl stretching frequency corresponding to the carboxylic acid groups (1709 cm^{-1}) has disappeared for the **AS** dyes (Figure S23, Supporting Information), which establish the coupling between the dye and TiO_2. The light harvesting efficiency (**LHE**) of the **AS** dyes has been calculated (LHE = 1−10^{-A}) at 80% and showed different

https://doi.org/10.1021/acsomega.4c00123
ACS Omega 2024, 9, 16429−16442

Table 1. Photophysical and Electrochemical Properties of AS1−AS5 Dyes along with Reference Dye AK2 at Room Temperature

dyes	λ_{max} (nm) CH_2Cl_2 [a]	λ_{max} (nm) CH_2Cl_2 [b]	ε (10^5 M^{-1} cm^{-1})	λ_{max} (nm) on TiO_2 [c]	LHE $\Delta\lambda$ at 80%(nm)	E_{ox} (V vs Ag/Ag^+)[d]	E_{HOMO} (V vs NHE)	E_{LUMO} (V vs NHE)	E_g (eV)[e]
AK2	530	572	1.84	485	174	0.439	0.98	−1.27	2.25
AS1	505	573	1.46	490	185	0.525	1.06	−1.21	2.27
AS2	518	572	1.61	502	143	0.487	1.03	−1.24	2.27
AS3	501	560	1.54	506	166	0.532	1.07	−1.27	2.34
AS4	509	576	1.53	505	188	0.545	1.08	−1.22	2.30
AS5	535	572	1.52	535	168	0.508	1.05	−1.20	2.25

[a]Absorption. [b]Emission of **AK2** and **AS1−5** dyes in CH_2Cl_2. [c]On TiO_2 (thickness 6 μm and dipping time 10 min). [d]Oxidation potentials were measured in CH_2Cl_2, where tetrabutylammonium perchlorate ($TBAClO_4$) used as a supporting electrolyte and Fc/Fc^+ used as an external standard and converted to NHE by addition of 0.7 V. [e]E_g optical band gap.

LHE properties due to the changed acceptor unit position and alkyl group incorporation (Figure 2c and Table 1). Here, the **AS2** dye showed a relatively narrowed LHE due to more hindrance near the anchoring group compared to other **AS** dyes. All the dyes belonging to the **AS** series showed reversible redox properties, where two oxidation and two reduction peaks have been obtained during the cyclic voltammetry experiment, and cyclic voltammograms for the **AS** dyes are provided in Figure S15. The differential pulse voltammetry (DPV) experiments were performed in an anhydrous CH_2Cl_2 solution to find out the redox potentials of the **AS** dyes (Figure 3a). **AS** dyes showed two oxidation peaks.**AS2** and **AS5** (dyes with shorter acceptor-anchoring group distance) that were oxidized easily compared to **AS1**, **AS3**, and **AS4** (dyes with longer acceptor-anchoring group distance). The first oxidation potential obtained from the DPV experiment for the **AS** dyes has been used to calculate the highest molecular occupied orbital (HOMO) energy level, where the oxidation potential converted with respect to NHE by the addition of 0.7 V (by using an external standard of ferrocene).[49] Intersection points of absorbance and emission spectra have been used to calculate the optical energy gap of the **AS** dyes by using the formula $E_g = 1240/\lambda_{intersection}$. Further, the lowest unoccupied molecular orbital (LUMO) energy levels of the **AS** dyes were calculated by subtracting the band gap from the HOMO of the dyes. The HOMO energy levels were estimated to be 1.06, 1.03, 1.07, 1.08, and 1.05 eV (vs NHE) for **AS1**−**AS5**, respectively, and the LUMO energy levels of the dyes were found to be −1.21, −1.24, −1.27, −1.20, and −1.27 eV (vs NHE) for **AS1**−**AS5**, respectively. The HOMO of **AS** dyes has sufficient over potential in the range of 0.63−0.68 V to the I^-/I_3^- electrolyte for the dye regeneration processes, and LUMO has sufficient negative potential in the range of −0.70 to −0.77 V compared to the TiO_2 conduction band level (−0.5 V vs NHE) for the electron injection processes.

Furthermore, the charge injection efficiency of photoexcited **AS** dyes to the conduction band of TiO_2 has been evaluated by steady-state fluorescence quenching experiments. **AS** dyes have been anchored on TiO_2 and insulating ZrO_2 surfaces, and a similar OD at the excitation wavelengths on both surfaces was maintained for the **AS** dyes. The efficiency of fluorescence quenching on the TiO_2 surface over the ZrO_2 surface has been used to evaluate the charge injection efficiency. The charge injection efficiency for the **AS** dyes was 75−79% (Figures S24 and S25, Supporting Information) which indicated the efficient charge separation process occurred at the dye−TiO_2 interface.

3.3. Computational Studies. All the DFT calculations were performed by employing Gaussian09 software[50] for **AS** dyes with changes in the position of the acceptor unit, using the B3LYP, 6-311G (++) level of theory, to assess the effect of acceptor unit position on electronic distributions in different electronic states. The isodensity surface value was fixed at 0.03 (Figure 4). For all the **AS** dyes, the HOMO electronic level showed the maximum electron density on the squaric acid unit, whereas the LUMO is significantly populated on the anchoring $-CO_2H$ group which help in unidirectional charge transfer from the photoexcited dye to the conduction band of TiO_2. Here, **AS1**, **AS3**, and **AS4** dyes with a similar π-backbone (long distance between the acceptor and carboxylic acid units) showed similar electronic distributions in the different electronic levels, but the dihedral angle changed in the **AS3** dye by incorporating the ethyl−hexyl chain at the An donor. The **AS2** and **AS5** dyes with a similar π-backbone (short distance between the acceptor and carboxylic acid units) showed slight variations in electronic

https://doi.org/10.1021/acsomega.4c00123
ACS Omega 2024, 9, 16429−16442

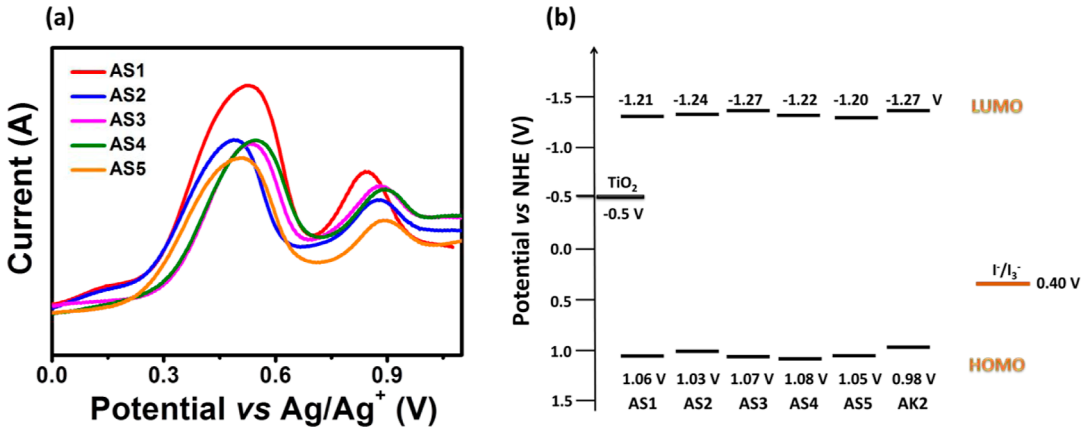

Figure 3. (a) Differential pulse voltammograms of **AS** dyes in CH_2Cl_2 solution and (b) energy level diagram of **AS1−5** dyes along with reference dye **AK2**.

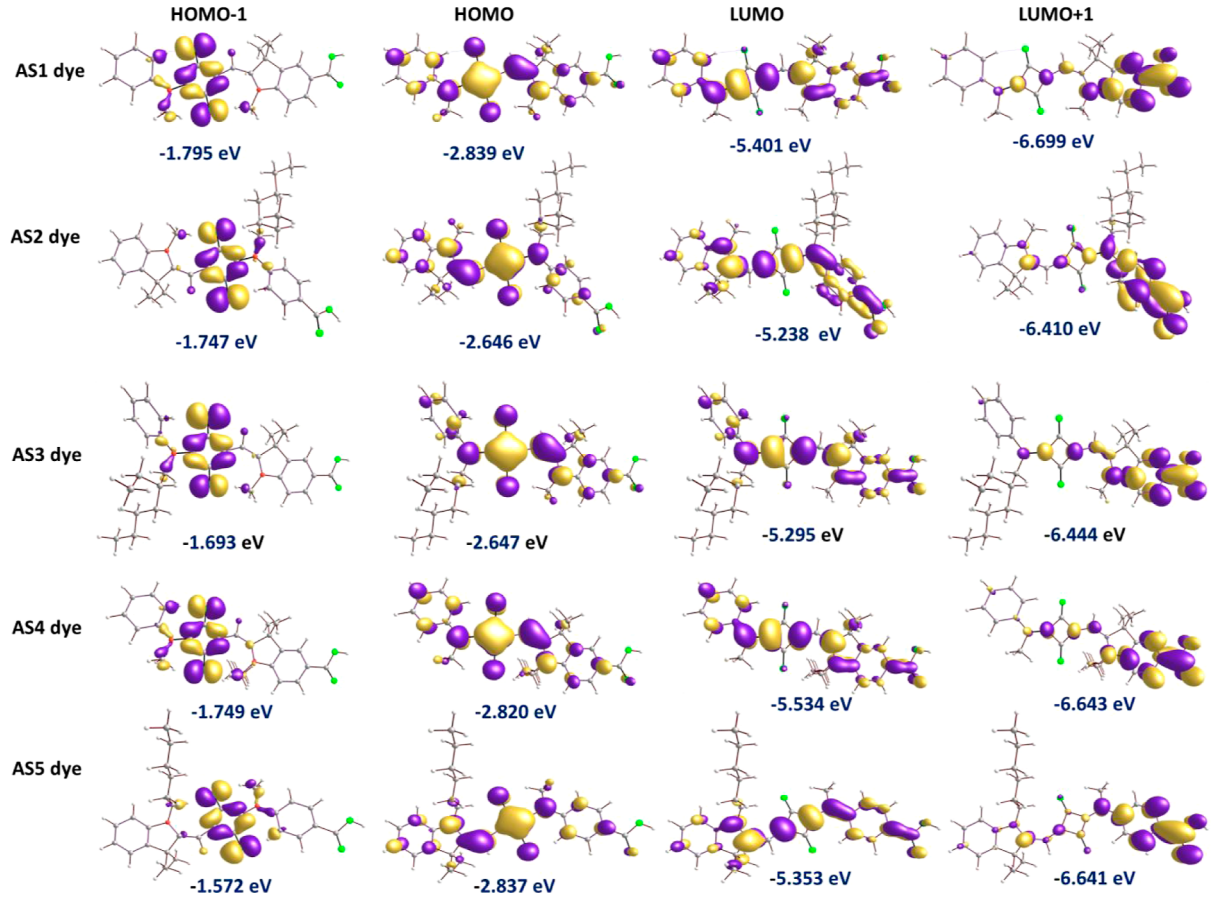

Figure 4. Energy-minimized frontier molecular orbital diagram of D−A−D-based **AS1**, **AS2**, **AS3**, **AS4**, and **AS5** dyes with their electronic levels.

distributions for the different electronic levels, and the dihedral angle of the **AS2** dye changed due to incorporating the ethyl−hexyl chain at the An donor. It has been observed that the branched N-alkylation of An and In donors disturbed the planarity of the molecule compared with the normal N-alkylation. Further, the dipole moment obtained from the energy-optimized structures for the long acceptor-anchoring group distance-based **AS1**, **AS3**, and **AS4** dyes was relatively low (1.96, 3.23, and 2.14 D, respectively) compared to the small acceptor-anchoring group distance-based **AS2** (5.40 D), **AS5** (6.77 D), and **AK2** (6.73 D) dyes. The dipole moment of the dyes increased with the An donor attached to the anchoring group (shorter distance) compared to the nonanchoring In donor unit due to the change in the electronic structures. The distance between the N atom of In and An donors and the carbonyl C atom of carboxylic acid and the acceptor unit was calculated from the minimized energy structure of molecules by DFT (Figure 5). The average lengths of visible light active **AS** dyes range from 15.5 to 16.6 Å, depending on the anchoring group position on donor units. Anchoring group attached to the An donor promotes the molecule to slightly twist, resulting in a decreased length compared to the anchoring group attached to the In donor. The distance between both carbonyl-C of the acceptor unit and carboxylic acid C═O of the anchoring group

https://doi.org/10.1021/acsomega.4c00123
ACS Omega 2024, 9, 16429−16442

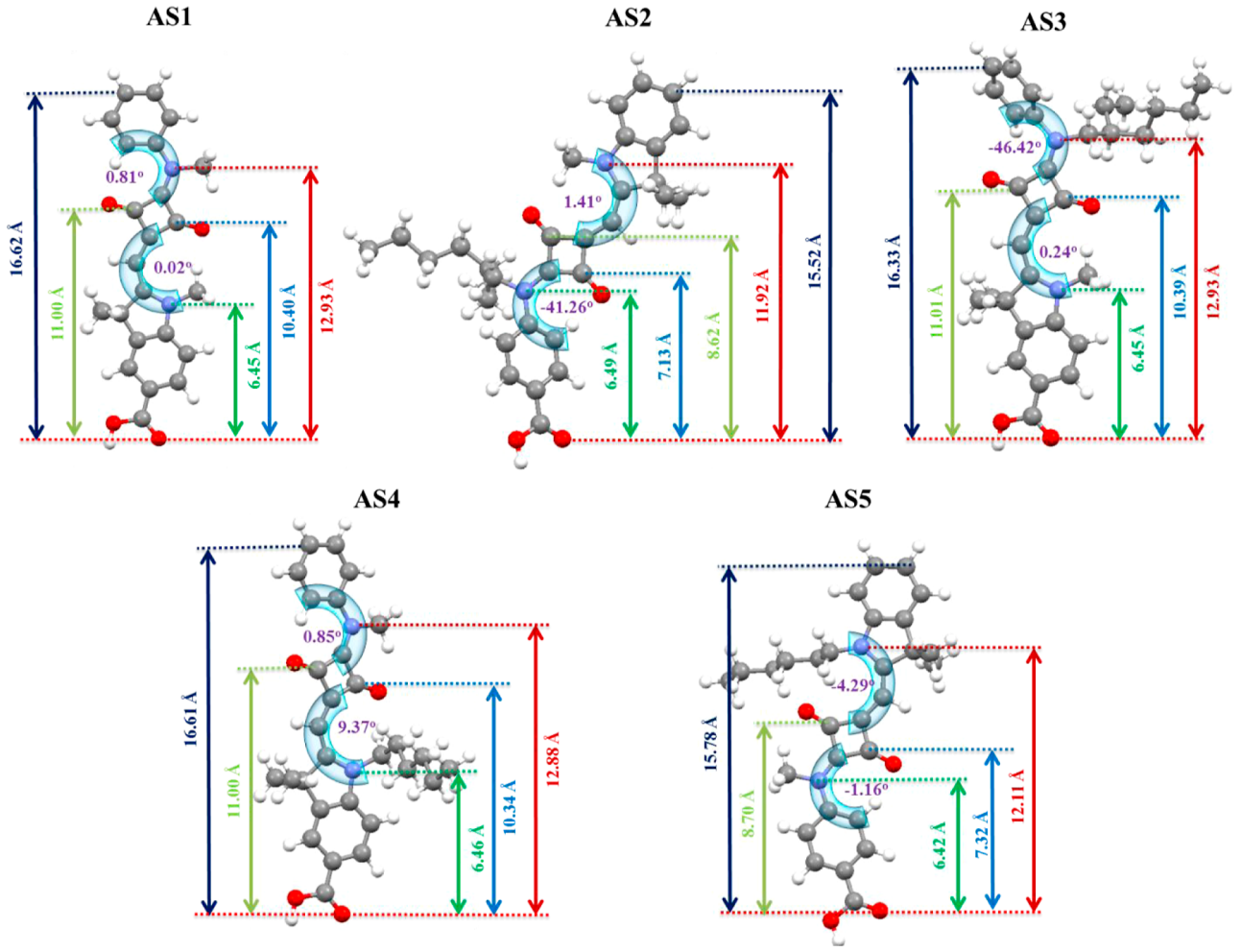

Figure 5. Energy-minimized structures of **AS1**−**AS5** dyes with structural features (distance between the carboxylic acid C═O of the anchoring group to the N atom of donors and the carbonyl-C atom of the squaraine acceptor) and dihedral angles between An and In donor and acceptor units.

was greater for **AS1** (10.4−11.0 Å), **AS3** (10.39−11.01 Å), and **AS4** (10.34−11.0 Å) dyes compared to **AS2** (7.13−8.62 Å) and **AS5** (7.32−8.70 Å) dyes. The dihedral angles between the An unit and acceptor unit in-plane were 0.81, −41.26, −46.42, 0.85, and −1.16° for the **AS1**, **AS2**, **AS3**, **AS4**, and **AS5** dyes, respectively, indicating that branching at the An donor distorted the geometry of the molecule.

3.4. Photovoltaic Performance. The DSSC device characterizations of the photoanode made from the **AS** dyes and **AK2** dye with the I^-/I_3^- electrolyte have been carried out, and optimized DSSC results have been provided in Figure 6 and Table 2. The DSSC device performance for **AS2**, **AS5**, and **AK2** dyes (with shorter acceptor-anchoring group distance) obtained was high compared to that for the **AS1**, **AS3**, and **AS4** dyes (with longer acceptor-anchoring group distance). The **AS1** dye with longer acceptor-anchoring group distance gave a V_{OC} of 768 mV, a J_{SC} of 9.46 mA cm^{-2}, and an efficiency of 5.49%, whereas the **AK2** dye (which is only different in respect to the donor position) gave a maximum V_{OC} of 802 mV, a J_{SC} of 11.90 mA cm^{-2}, and an efficiency of 7.51% in the absence of CDCA. Similarly, device performance patterns have been observed between **AS3**/**AS2** and **AS4**/**AS5** dyes in the absence of CDCA, which indicates that the charge injection enhanced with the small acceptor-anchoring group distance without steric hindrance. Incorporation of an ethyl−hexyl group into the An unit near the TiO_2 surface for the **AS2** dye enhanced the V_{OC} by passivating the TiO_2 surface and reduced the J_{SC} (dye loading on TiO_2) and DSSC efficiency compared to the **AK2** dye. Fabrication of DSSC devices of **AS** dyes with 2 equiv of CDCA enhanced the V_{OC} of all the dyes due to better TiO_2 passivation from the oxidized electrolytes (by minimizing the charge recombination between oxidized electrolytes and electrons present into conduction band of TiO_2). However, the J_{SC} of **AS** dyes (except the **AS5** dye) decreased when the dyes were sensitized with CDCA. Meanwhile, the J_{SC} was found to be high for shorter distance of acceptor-CO_2H dyes **AS5** and **AK2**, but a decrease in the case of **AS2** due to the branched alkyl group near TiO_2 leads to low dye loading without CDCA. However, dyes with long distance acceptor units **AS1**, **AS3**, and **AS4** showed little difference in J_{SC} value, but the **AS1** dye has high dye loading and showed low J_{SC} value due to aggregation and charge recombination (Figure S16g and Table S3). Here, the **AS5** dye sensitized with 2 equiv of CDCA showed a maximum DSSC device efficiency of 8.01% with a V_{OC} of 819 mV and a J_{SC} of 11.98 mA cm^{-2} compared to reference **AK2** and other **AS** dyes. Here, visible light-responsive unsymmetrical squaraine dyes **AS** with the N-hexylation on the In moiety that is away from the TiO_2 surface showed a significant effect on the DSSC device performance compared to the N-alkylation on the An moiety that is near or away from the TiO_2 surface. **AS** dyes with a small acceptor-anchoring group distance showed a better IPCE response over the dyes with a longer acceptor-anchoring group

https://doi.org/10.1021/acsomega.4c00123
ACS Omega 2024, 9, 16429−16442

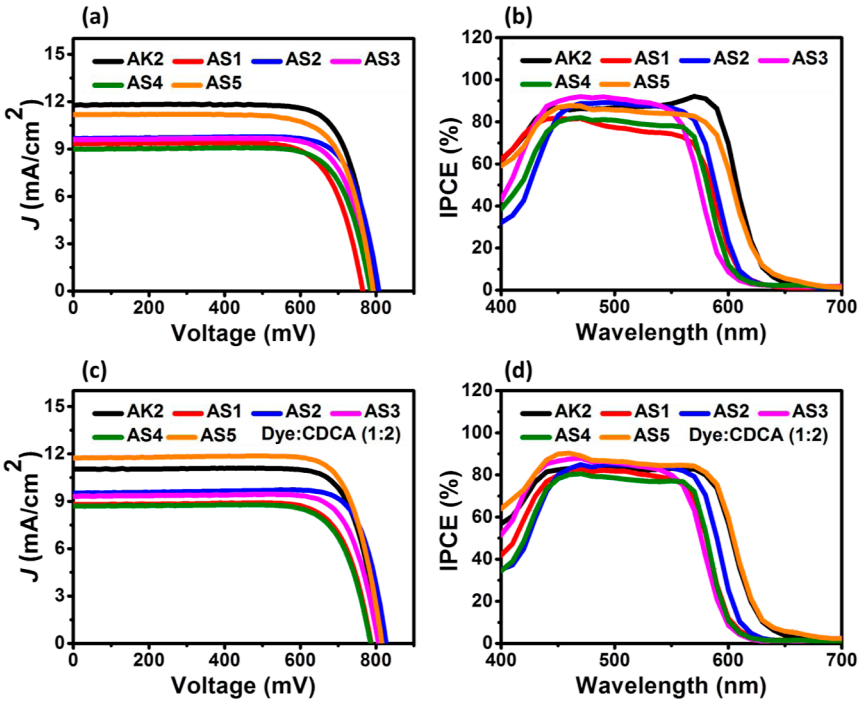

Figure 6. (a) *I*–*V* and (b) IPCE curves for **AK2** and **AS** dyes without CDCA, (c) *I*–*V*, and (d) IPCE curves for **AK2** and **AS** dyes with CDCA in the I^-/I_3^- electrolyte.

Table 2. Optimized DSSC Performances of AS and AK2 dyes with and without the Coadsorbent (CDCA) in the I^-/I_3^- Electrolyte

dyes	CDCA	V_{OC} (mV)	J_{SC} (mA/cm^2)	ff (%)	η (%)
AK2	0	800 ± 2	11.76 ± 0.14	78 ± 0.68	7.34 ± 0.17
AK2	2	812 ± 1	11.03 ± 0.27	80 ± 0.95	7.17 ± 0.27
AS1	0	765 ± 3	9.34 ± 0.12	75 ± 0.59	5.36 ± 0.13
AS1	2	787 ± 4	8.80 ± 0.18	78 ± 0.67	5.40 ± 0.19
AS2	0	808 ± 2	9.69 ± 0.16	79 ± 0.43	6.19 ± 0.15
AS2	2	827 ± 2	9.53 ± 0.19	82 ± 0.83	6.46 ± 0.21
AS3	0	791 ± 4	9.59 ± 0.23	78 ± 0.82	5.92 ± 0.24
AS3	2	807 ± 3	9.32 ± 0.21	79 ± 0.78	5.94 ± 0.22
AS4	0	786 ± 3	9.01 ± 0.17	76 ± 0.94	5.38 ± 0.19
AS4	2	805 ± 2	8.70 ± 0.10	78 ± 0.64	5.46 ± 0.13
AS5	0	793 ± 3	11.19 ± 0.25	77 ± 0.61	6.83 ± 0.23
AS5	2	816 ± 3	11.74 ± 0.24	81 ± 0.56	7.76 ± 0.25

distance. Incorporation of the *N*-ethylhexyl group in the An moiety of the **AS2** dye showed decreased IPCE response, whereas N-hexylation on the In moiety for the **AS5** dye showed enhanced IPCE response which was further enhanced by CDCA addition compared to the **AS2** dye. The V_{OC} of the DSSC devices changed due to shifts in the conduction band of TiO_2 due to the dipole moment of dyes.[51,52] It is observed that the V_{OC} for the DSSC devices sensitized with the dyes with An-SQ-In-CO_2H (longer distance between the SQ unit and the anchoring group) was lower than its other counterpart (In-SQ-An-CO_2H), and it may be due to the reduced dipole moments of the earlier set of dyes (Table S4, Supporting Information). Further, the presence of the alkyl group away from the TiO_2 surface helps more loading of dyes compared to the dyes with the alkyl group, which is near to the surface. Overall, the influence of alkyl groups can be discussed in two aspects: (i) the effect of position of the alkyl group, whether near or far away to the $-CO_2H$ anchoring group, and (ii) the effect of linear vs branched alkyl groups. Dyes **AS5**, **AS3** and **AS4**, **AS2** have alkyl groups away and near the anchoring groups, respectively. Alkyl groups near the anchoring group may shield the 5-coordinated Ti site which affects the dye loading capacity that affects the

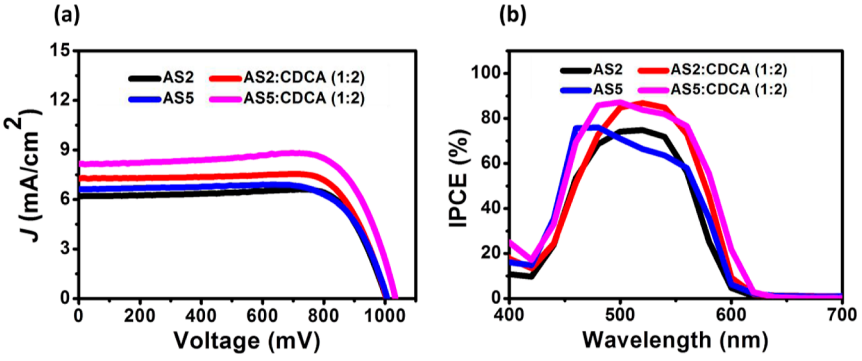

Figure 7. (a) *I*–*V* and (b) IPCE curves for **AS2** and **AS5** dyes in the presence and absence of CDCA with the Cu(I/II) electrolyte.

https://doi.org/10.1021/acsomega.4c00123
ACS Omega 2024, 9, 16429−16442

Table 3. Optimized DSSC Performances of AS2 and AS5 dyes in the Presence and Absence of the Coadsorbent (CDCA) with the Cu(I/II) Electrolyte

dyes	electrolyte	V_{OC} (mV)	J_{SC} (mA/cm^2)	ff (%)	η (%)
AS2	Cu(I/II)	1004 ± 2	6.21 ± 0.09	82 ± 0.88	5.11 ± 0.14
AS2/CDCA(1:2)	Cu(I/II)	1005 ± 2	7.27 ± 0.11	79 ± 1.03	5.77 ± 0.18
AS5	Cu(I/II)	1007 ± 3	6.63 ± 0.15	77 ± 0.93	5.14 ± 0.20
AS5/CDCA(1:2)	Cu(I/II)	1034 ± 2	8.16 ± 0.20	81 ± 0.72	6.84 ± 0.24

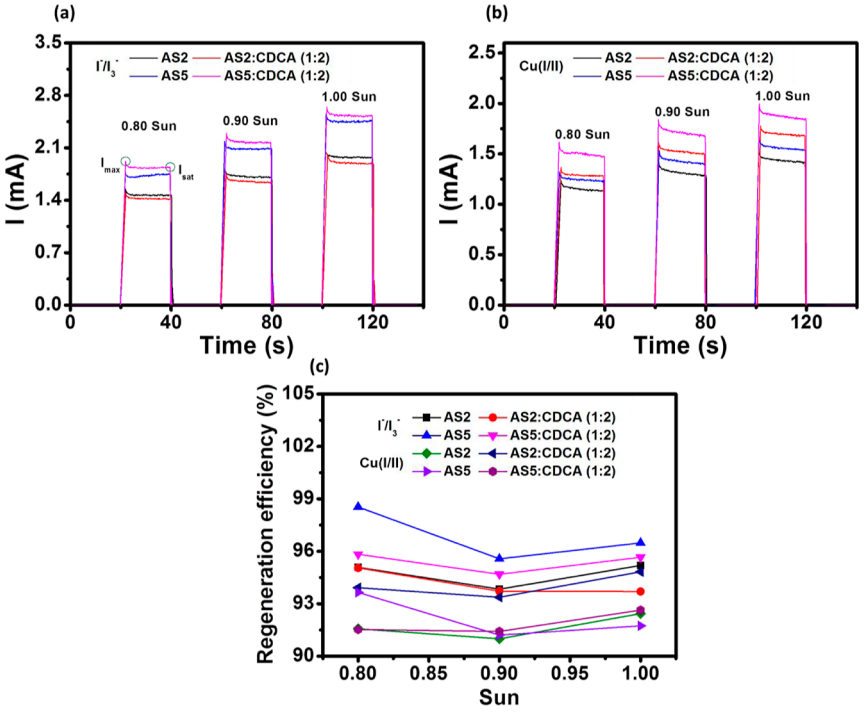

Figure 8. Current transient profile of **AS2** and **AS5** dyes with the (a) I^-/I_3^- electrolyte and (b) Cu (I/II) electrolyte and (c) regeneration efficiency of **AS2** and **AS5** dyes with I^-/I_3^- and Cu (I/II) electrolytes at different sun intensities.

device performance (Table S3, Supporting Information), whereas alkyl groups enhance the dye−dye interaction when it is functionalized slightly far away from the anchoring groups for better dye loading. Hence, **AS5** and **AS3** are performing better than **AS2** and **AS4** dyes, respectively.

Furthermore, introducing linear and branched alkyl groups at the N atoms of In and An donors may affect the planarity of the dyes. The presence of alkyl groups on the N atom of the An donor distorts the dye structures more than that of having the alkyl group on the N atom of the In unit. It is possible that more distortion on the planarity of the structure is due to the alkylated N atom of the An donor being directly attached to the four-membered cyclic squaric acid unit. Hence, the dihedral angle between the N-alkylated An donor and squaric acid acceptor is more than that of the N-alkylated In donor and squaric acid acceptor (Figure 5). While comparing the device performance of **AS5** and **AS3** (both dyes possess alkyl groups on the top), the **AS5** dye performs better than **AS3**.

Furthermore, the HOMO energy level of the highly efficient **AS2** and **AS5** dyes was more positive and therefore has been tested with the copper electrolyte. The DSSC device characterizations of the photoanode made from **AS2** and **AS5** dyes in the Cu(I/II) electrolyte with and without CDCA have been carried out, and optimized DSSC results have been provided in Figure 7 and Table 3. Here, the **AS5** dye gave the highest V_{OC} of 1036 mV, a J_{SC} of 8.36 mA cm^{-2}, and an efficiency of 7.08%, whereas the **AS2** dye gave a V_{OC} of 1007 mV, a J_{SC} of 7.38 mA cm^{-2}, and an efficiency of 5.95% with 2 equiv of CDCA. The V_{OC} of 1010 mV, J_{SC} of 6.78 mA cm^{-2}, and efficiency of 5.34% have been achieved by the **AS5** dye, whereas 1006 mV of V_{OC}, 6.30 mAcm^{-2} of J_{SC}, and 5.25% efficiency have been achieved by the **AS2** dye in the absence of CDCA. Further, the integrated J_{SC} value obtained from IPCE is matched with the J_{SC} value obtained from the $I-V$ characterization with the I^-/I_3^- electrolyte and Cu (I/II) electrolyte for **AS** dyes (Tables S1 and S2)).

The mass transport limitations were determined by the photocurrent transient experiment (Figure 8). Here, we have selected the highly efficient dye, **AS5**, along with the **AS2** dye for the transient experiment with I^-/I_3^- and Cu(I/II) electrolytes. The current values increased along with a light illumination intensity of 0.8 Sun to 1.0 Sun. Here, **AS2** and **AS5** dyes with the Cu(I/II) electrolyte showed relatively low current compared to the I^-/I_3^- electrolyte and supports the current obtained from $I-V$ characterization. Further, the regeneration efficiency of the **AS2** and **AS5** dyes was calculated, which showed >90% with both electrolytes.

3.5. Electrochemical Impedance Spectroscopy. Charge recombination resistance (R_{ct}), chemical capacitance (C_μ), and lifetime of electrons (τ) in TiO_2 are the important parameters to study the dye−TiO_2/electrolyte interface in a DSSC device and determine the device performance, and high values of these

https://doi.org/10.1021/acsomega.4c00123
ACS Omega 2024, 9, 16429−16442

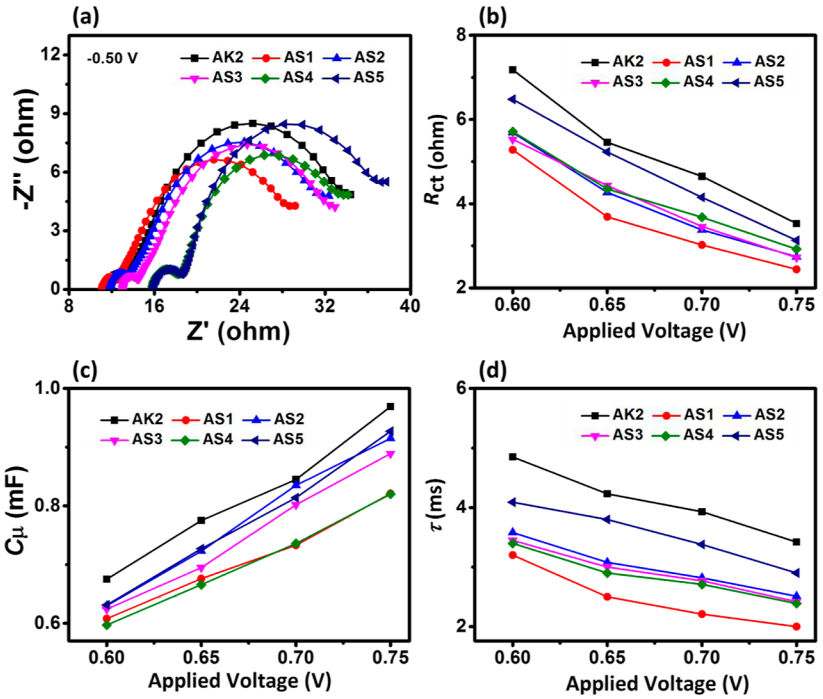

Figure 9. (a) Nyquist plot, (b) charge recombination resistance, (c) chemical capacitance, and (d) lifetime of electrons of **AK2** and **AS** dyes without CDCA.

parameters directly reflect the DSSC device efficiency. All the above parameters can be captured by performing the electrochemical impedance spectroscopy (EIS) experiment. To scrutinize the device efficiency of In-An donor-based **AS** and **AK2** dyes with the I^-/I_3^- electrolyte, EIS characterizations were carried out in dark conditions by applying the different potentials (Figures S17−S21).[53] The Nyquist plots for **AS** dyes along with reference dye **AK2** without CDCA at 0.5 V applied potentials are shown in Figure 9a. The R_{ct} and C_μ values were obtained by fitting the Nyquist plot, and multiplication of these two parameters gave the τ value. The order of R_{ct} values without CDCA are 5.28 Ω (**AS1**) < 5.53 Ω (**AS3**) < 5.70 Ω (**AS2**) < 5.71 Ω (**AS4**) < 6.48 Ω (**AS5**) < 7.18 Ω (**AK2**) which were further changed in the order 5.49 Ω (**AS1**) < 5.59 Ω (**AS2**) < 5.69 Ω (**AS3**) < 5.95 Ω (**AS4**) < 6.38 Ω (**AK2**) < 8.86 Ω (**AS5**) with CDCA by sensitizing the dyes with CDCA. The R_{ct} values for the devices fabricated with **AS1**, **AS3**, and **AS4** dyes were low when the distance between the acceptor units and anchoring group was large compared to the short distance between the acceptor and $-CO_2H$ group of **AS2** and **AS5** without CDCA. However, the R_{ct} of the **AS2** dye decreased because the branched alkyl group position was down (near to the TiO_2 surface). The low R_{ct} for the **AS5** dye without CDCA compared to the **AK2** dye is due to the unwanted vacant spaces between the anchored **AS5** dyes which aroused due to the steric hindrance on TiO_2. The spaces between the **AS5** dyes were filled by CDCA molecules, which passivated the TiO_2 surface from the oxidized electrolyte and enhanced the R_{ct} compared to **AK2** (increased competition between dye and CDCA anchoring). Further, it has been observed that the branched alkyl groups at up and down positions showed poor response over the normal alkyl groups with or without CDCA, whereas the short distance acceptor unit depicted good response due to the increase in the interfacial electron process with TiO_2. Similarly, chemical capacitance (C_μ) and lifetime (τ) values were obtained high for **AK2** (6.728 D) without CDCA and for **AS5** (6.77 D) with CDCA and supports the achieved efficiency for the respective dyes (Table 4). The obtained high C_μ values for **AK2** and **AS5**

Table 4. EIS Parameters of the DSSC Device Made with Reference Dyes AK2 and AS Dyes in the Dark with an Applied Potential of 0.60 V

dye	R_{ct} (ohm)	C_μ (mF)	τ (ms)
AK2	7.18	0.675	4.85
AK2/CDCA(1:2)	6.38	0.648	4.13
AS1	5.28	0.608	3.20
AS1/CDCA(1:2)	5.49	0.617	3.38
AS2	5.70	0.630	3.58
AS2/CDCA(1:2)	5.59	0.628	3.50
AS3	5.53	0.624	3.45
AS3/CDCA(1:2)	5.69	0.606	3.44
AS4	5.71	0.597	3.40
AS4/CDCA(1:2)	5.95	0.618	3.67
AS5	6.48	0.631	4.09
AS5/CDCA(1:2)	8.86	0.734	6.50

are due to the change in dipole moment and revealed the importance of small acceptor-anchoring group distance over the longer distance, whereas the value revealed the high achieved current and voltage for the respective dyes. The conduction band, E_{CB}, depends on the dipole moment (μ) of the dye (eq 1). The E_{CB} is directly proportional to the dipole moment, so when the dipole moment of the sensitizer increases the E_{CB} upshift resultant, the V_{OC} also increased.[50]

$$\Delta E_{CB} = -\frac{q\mu\gamma}{\varepsilon_o\varepsilon} \quad (1)$$

4. CONCLUSIONS

In summary, a series of unsymmetrical squaraine dyes **AS1**−**AS5** with changes in the position of In and An units along with a less

https://doi.org/10.1021/acsomega.4c00123
ACS Omega 2024, 9, 16429−16442

hindered alkyl group have been designed and synthesized for DSSCs. The isomeric **AS** dyes showed varied absorption properties due to the change in the position of In and An units and alkyl groups. The UV−vis absorption of long acceptor-anchoring group distance for the **AS1**, **AS3**, and **AS4** dyes (An-SQ-In-CO_2H) showed a blue shift compared to the short acceptor-anchoring group distance for the **AS2** and **AS5** dyes (In-SQ-An-CO_2H) in CH_2Cl_2. The dihedral angles between the An and squaraine units were high, −41.26° and −46.42° for AS2 and **AS3** dyes, respectively, due to the presence of branched alkyl groups at the An unit compared to the normal alkyl chain-containing dyes **AS4** (0.85°) and **AS5** (−1.16°). The DSSC device performance for the **AS** dyes showed the importance of short acceptor-anchoring groups over a long distance for better device performance. The maximum DSSC device efficiency of 8.01% has been achieved for the **AS5** dye with CDCA in the I^-/I_3^- electrolyte. Further, the **AS5** dye sensitized with CDCA gave the highest V_{OC} of 1036 mV, J_{SC} of 8.36 mAcm^{-2}, and efficiency of 7.08% with the Cu(I/II) electrolyte. The obtained results from these sets of dyes revealed the importance of acceptor-anchoring group distance on photovoltaic performance and will be useful for further designing the new squaraine-based dyes for DSSCs.

■ ASSOCIATED CONTENT

Supporting Information

The Supporting Information is available free of charge at https://pubs.acs.org/doi/10.1021/acsomega.4c00123.

General methods, DSSC device fabrication, ^1H and ^{13}C NMR, mass, EIS, and dye-desorption study of AS dyes (PDF)

■ AUTHOR INFORMATION

Corresponding Authors

Kothandam Krishnamoorthy − *Polymer Science and Engineering Division, CSIR-National Chemical Laboratory, Pune 411008, India; Academy of Scientific and Innovative Research (AcSIR), Ghaziabad 201002, India;* orcid.org/0000-0003-0603-8694; Email: k.krishnamoorthy@ncl.res.in

Jayaraj Nithyanandhan − *Physical and Materials Chemistry Division, CSIR-National Chemical Laboratory, Pune 411008, India; Academy of Scientific and Innovative Research (AcSIR), Ghaziabad 201002, India;* orcid.org/0000-0002-3429-4989; Email: j.nithyanandhan@ncl.res.in

Authors

Amrita Singh − *Physical and Materials Chemistry Division, CSIR-National Chemical Laboratory, Pune 411008, India; Academy of Scientific and Innovative Research (AcSIR), Ghaziabad 201002, India*

Ambarish Kumar Singh − *Physical and Materials Chemistry Division, CSIR-National Chemical Laboratory, Pune 411008, India; Academy of Scientific and Innovative Research (AcSIR), Ghaziabad 201002, India*

Ruchi Dixit − *Physical and Materials Chemistry Division, CSIR-National Chemical Laboratory, Pune 411008, India; Academy of Scientific and Innovative Research (AcSIR), Ghaziabad 201002, India*

Kumar Vanka − *Physical and Materials Chemistry Division, CSIR-National Chemical Laboratory, Pune 411008, India; Academy of Scientific and Innovative Research (AcSIR), Ghaziabad 201002, India;* orcid.org/0000-0001-7301-7573

Complete contact information is available at: https://pubs.acs.org/10.1021/acsomega.4c00123

Author Contributions

The manuscript was written through contributions of all authors. All authors have given approval to the final version of the manuscript.

Notes

The authors declare no competing financial interest.

■ ACKNOWLEDGMENTS

This work was financially supported by SERB, India (CRG/2020/003105), and the Council of Scientific and Industrial Research (CSIR), India (NWP0054, CSIR-TAPSUN). A.S. thanks UGC for the JRF research fellowship, and A.K.S. and R.D. thanks CSIR, New Delhi, India, for the research fellowships.

■ REFERENCES

(1) Hagfeldt, A.; Boschloo, G.; Sun, L.; Kloo, L.; Pettersson, H. Dye-Sensitized Solar Cells. *Chem. Rev.* **2010**, *110*, 6595−6663.

(2) Gratzel, M. Recent Advances in Sensitized Mesoscopic Solar Cells. *Acc. Chem. Res.* **2009**, *42*, 1788−1798.

(3) Wu, J.; Lan, Z.; Lin, J.; Huang, M.; Huang, Y.; Fan, L.; Luo, G. Electrolytes in Dye-Sensitized Solar Cells. *Chem. Rev.* **2015**, *115*, 2136−2173.

(4) Ji, J. M.; Zhou, H.; Kim, H. K. Rational Design Criteria for D-π-A Structured Organic and Porphyrin Sensitizers for Highly Efficient Dye-Sensitized Solar Cells. *J. Mater. Chem. A* **2018**, *6*, 14518−14545.

(5) O'Regan, B.; Gratzel, M. A Low-Cost, High-Efficiency Solar Cell Based on Dye-Sensitized Colloidal TiO_2 Films. *Nature* **1991**, *353*, 737−740.

(6) Beard, M. C.; Luther, J. M.; Semonin, O. E.; Nozik, A. J. Third Generation Photovoltaics Based on Multiple Exciton Generation in Quantum Confined Semiconductors. *Acc. Chem. Res.* **2013**, *46*, 1252−1260.

(7) Hora, C.; Santos, F.; Sales, M. G. F.; Ivanou, D.; Mendes, A. Dye-Sensitized Solar Cells for Efficient Solar and Artificial Light Conversion. *ACS Sustain. Chem. Eng.* **2019**, *7*, 13464−13470.

(8) Zeng, K.; Tong, Z.; Ma, L.; Zhu, W. H.; Wu, W.; Xie, Y.; Xie, Y. Molecular Engineering Strategies for Fabricating Efficient Porphyrin-Based Dye-Sensitized Solar Cells. *Energy Environ. Sci.* **2020**, *13*, 1617−1657.

(9) Devadiga, D.; Selvakumar, M.; Shetty, P.; Santosh, M. S. Dye-Sensitized Solar Cell for Indoor Applications: A Mini-Review. *J. Electron. Mater.* **2021**, *50*, 3187−3206.

(10) Jilakian, M.; Ghaddar, T. H. Eco-Friendly Aqueous Dye-Sensitized Solar Cell with a Copper(I/II) Electrolyte System: Efficient Performance under Ambient Light Conditions. *ACS Appl. Energy Mater.* **2022**, *5*, 257−265.

(11) Freitag, M.; Teuscher, J.; Saygili, Y.; Zhang, X.; Giordano, F.; Liska, P.; Hua, J.; Zakeeruddin, S. M.; Moser, J. E.; Grätzel, M.; Hagfeldt, A. Dye-Sensitized Solar Cells for Efficient Power Generation under Ambient Lighting. *Nat. Photonics* **2017**, *11*, 372−378.

(12) Zhang, D.; Stojanovic, M.; Ren, Y.; Cao, Y.; Eickemeyer, F. T.; Socie, E.; Vlachopoulos, N.; Moser, J. E.; Zakeeruddin, S. M.; Hagfeldt, A.; Grätzel, M. A Molecular Photosensitizer Achieves a V_{OC} of 1.24 V Enabling Highly Efficient and Stable Dye-Sensitized Solar Cells with Copper(II/I)-Based Electrolyte. *Nat. Commun.* **2021**, *12*, 1777−1811.

(13) Bai, J.; Zhou, B. Titanium Dioxide Nanomaterials for Sensor Applications. *Chem. Rev.* **2014**, *114*, 10131−10176.

(14) Muñoz-García, A. B.; Benesperi, I.; Boschloo, G.; Concepcion, J. J.; Delcamp, J. H.; Gibson, E. A.; Meyer, G. J.; Pavone, M.; Pettersson,

H.; Hagfeldt, A.; Freitag, M. Dye-Sensitized Solar Cells Strike Back. *Chem. Soc. Rev.* **2021**, *50*, 12450−12550.
(15) Zhou, N.; Prabakaran, K.; Lee, B.; Chang, S. H.; Harutyunyan, B.; Guo, P.; Butler, M. R.; Timalsina, A.; Bedzyk, M. J.; Ratner, M. A.; Vegiraju, S.; Yau, S.; Wu, C. G.; Chang, R. P. H.; Facchetti, A.; Chen, M. C.; Marks, T. J. Metal-Free Tetrathienoacene Sensitizers for High-Performance Dye-Sensitized Solar Cells. *J. Am. Chem. Soc.* **2015**, *137*, 4414−4423.
(16) Eom, Y. K.; Kang, S. H.; Choi, I. T.; Yoo, Y.; Kim, J.; Kim, H. K. Significant Light Absorption Enhancement by a Single Heterocyclic Unit Change in the π-Bridge Moiety from Thieno[3,2-b]-Benzothiophene to Thieno[3,2-b]Indole for High Performance Dye-Sensitized and Tandem Solar Cells. *J. Mater. Chem. A* **2017**, *5*, 2297−2308.
(17) Mathew, S.; Yella, A.; Gao, P.; Humphry-Baker, R.; Curchod, B. F. E.; Ashari-Astani, N.; Tavernelli, I.; Rothlisberger, U.; Nazeeruddin, M. K.; Grätzel, M. Dye-Sensitized Solar Cells with 13% Efficiency Achieved through the Molecular Engineering of Porphyrin Sensitizers. *Nat. Chem.* **2014**, *6*, 242−247.
(18) Yu, Q.; Wang, Y.; Yi, Z.; Zu, N.; Zhang, J.; Zhang, M.; Wang, P. High-Efficiency Dye-Sensitized Solar Cells: The Influence of Lithium Ions on Exciton Dissociation, Charge Recombination, and Surface States. *ACS Nano* **2010**, *4*, 6032−6038.
(19) Zhang, L.; Yang, X.; Wang, W.; Gurzadyan, G. G.; Li, J.; Li, X.; An, J.; Yu, Z.; Wang, H.; Cai, B.; Hagfeldt, A.; Sun, L. 13.6% Efficient Organic Dye-Sensitized Solar Cells by Minimizing Energy Losses of the Excited State. *ACS Energy Lett.* **2019**, *4*, 943−951.
(20) Ren, Y.; Zhang, D.; Suo, J.; Cao, Y.; Eickemeyer, F. T.; Vlachopoulos, N.; Zakeeruddin, S. M.; Hagfeldt, A.; Grätzel, M. Hydroxamic Acid Pre-Adsorption Raises the Efficiency of Cosensitized Solar Cells. *Nature* **2023**, *613*, 60−65.
(21) Chen, C.; Nguyen, V. S.; Chiu, H.; Chen, Y.; Wei, T.; Yeh, C. Anthracene-Bridged Sensitizers for Dye-Sensitized Solar Cells with 37% Efficiency under Dim Light. *Adv. Energy Mater.* **2022**, *12*, 2104051.
(22) Fakharuddin, A.; Jose, R.; Brown, T. M.; Fabregat-Santiago, F.; Bisquert, J. A Perspective on the Production of Dye-Sensitized Solar Modules. *Energy Environ. Sci.* **2014**, *7*, 3952−3981.
(23) Yao, Z.; Wu, H.; Li, Y.; Wang, J.; Zhang, J.; Zhang, M.; Guo, Y.; Wang, P. Dithienopicenocarbazole as the Kernel Module of Low-Energy-Gap Organic Dyes for Efficient Conversion of Sunlight to Electricity. *Energy Environ. Sci.* **2015**, *8*, 3192−3197.
(24) Yao, Z.; Zhang, M.; Wu, H.; Yang, L.; Li, R.; Wang, P. Donor/Acceptor Indenoperylene Dye for Highly Efficient Organic Dye-Sensitized Solar Cells. *J. Am. Chem. Soc.* **2015**, *137*, 3799−3802.
(25) Wu, Y.; Zhu, W. Organic Sensitizers from D-π-A to D-A-π-A: Effect of the Internal Electron-Withdrawing Units on Molecular Absorption, Energy Levels and Photovoltaic Performances. *Chem. Soc. Rev.* **2013**, *42*, 2039−2058.
(26) Yao, Z.; Wu, H.; Li, Y.; Wang, J.; Zhang, J.; Zhang, M.; Guo, Y.; Wang, P. Dithienopicenocarbazole as the Kernel Module of Low-Energy-Gap Organic Dyes for Efficient Conversion of Sunlight to Electricity. *Energy Environ. Sci.* **2015**, *8*, 3192−3197.
(27) Singh, A. K.; Nithyanandhan, J. Indoline-Based Donor-π-Acceptor Visible-Light Responsive Organic Dyes for Dye-Sensitized Solar Cells: Co-Sensitization with Squaraine Dye for Panchromatic IPCE Response. *ACS Appl. Energy Mater.* **2022**, *5*, 1858−1868.
(28) Chai, Q.; Li, W.; Liu, J.; Geng, Z.; Tian, H.; Zhu, W. H. Rational Molecular Engineering of Cyclopentadithiophene-Bridged D-A-π-A Sensitizers Combining High Photovoltaic Efficiency with Rapid Dye Adsorption. *Sci. Rep.* **2015**, *5*, 11330−11411.
(29) Park, J. H.; Nam, D. G.; Kim, B. M.; Jin, M. Y.; Roh, D. H.; Jung, H. S.; Ryu, D. H.; Kwon, T. H. Planar D-Dπ-A Organic Sensitizers for Thin-Film Photoanodes. *ACS Energy Lett.* **2017**, *2*, 1810−1817.
(30) Chai, Z.; Wang, J.; Xie, Y.; Lin, P.; Li, H.; Chang, K.; Xu, T.; Mei, A.; Peng, Q.; Wang, M.; Han, H.; Li, Q.; Li, Z. Modulation of Acceptor Position in Organic Sensitizers: The Optimization of Intramolecular and Interfacial Charge Transfer Processes. *ACS Appl. Mater. Interfaces* **2019**, *11*, 27648−27657.
(31) Li, H.; Fang, M.; Tang, R.; Hou, Y.; Liao, Q.; Mei, A.; Han, H.; Li, Q.; Li, Z. The Introduction of Conjugated Isolation Groups into the Common Acceptor Cyanoacrylic Acid: An Efficient Strategy to Suppress the Charge Recombination in Dye Sensitized Solar Cells and the Dramatically Improved Efficiency from 5.89% to 9.44%. *J. Mater. Chem. A* **2016**, *4*, 16403−16409.
(32) Xiang, W.; Gupta, A.; Kashif, M. K.; Duffy, N.; Bilic, A.; Evans, R. A.; Spiccia, L.; Bach, U. Cyanomethylbenzoic Acid: An Acceptor for Donor-π-Acceptor Chromophores Used in Dye-Sensitized Solar Cells. *ChemSusChem* **2013**, *6*, 256−260.
(33) Chai, Z.; Wan, S.; Zhong, C.; Xu, T.; Fang, M.; Wang, J.; Xie, Y.; Zhang, Y.; Mei, A.; Han, H.; Peng, Q.; Li, Q.; Li, Z. Conjugated or Broken: The Introduction of Isolation Spacer Ahead of the Anchoring Moiety and the Improved Device Performance. *ACS Appl. Mater. Interfaces* **2016**, *8*, 28652−28662.
(34) Qin, C.; Wong, W. Y.; Han, L. Squaraine Dyes for Dye-Sensitized Solar Cells: Recent Advances and Future Challenges. *Chem.—Asian J.* **2013**, *8*, 1706−1719.
(35) Singh, A. K.; Mele Kavungathodi, M. F.; Nithyanandhan, J. Alkyl-Group-Wrapped Unsymmetrical Squaraine Dyes for Dye-Sensitized Solar Cells: Branched Alkyl Chains Modulate the Aggregation of Dyes and Charge Recombination Processes. *ACS Appl. Mater. Interfaces* **2020**, *12*, 2555−2565.
(36) Singh, A.; Singh, A. K.; Dixit, R.; Vanka, K.; Krishnamoorthy, K.; Jayaraj, N. Visible-Light Active Unsymmetrical Squaraine Dyes with 1 V of Open-Circuit Voltage For Dye-sensitized Solar Cell. *ChemPhotoChem* **2023**, *7*, No. e202200328.
(37) Bisht, R.; Sudhakar, V.; Mele Kavungathodi, M. F.; Karjule, N.; Nithyanandhan, J. Fused Fluorenylindolenine-Donor-Based Unsymmetrical Squaraine Dyes for Dye-Sensitized Solar Cells. *ACS Appl. Mater. Interfaces* **2018**, *10*, 26335−26347.
(38) Karjule, N.; Munavvar, M. F.; Nithyanandhan, J. Heterotriangulene-Based Unsymmetrical Squaraine Dyes: Synergistic Effects of Donor Moieties and out-of-Plane Branched Alkyl Chains on Dye Cell Performance. *J. Mater. Chem. A* **2016**, *4*, 18910−18921.
(39) de Miguel, G.; Ziolek, M.; Zitnan, M.; Organero, J. A.; Pandey, S. S.; Hayase, S.; Douhal, A. Photophysics of H- and J-Aggregates of Indole-Based Squaraines in Solid State. *J. Phys. Chem. C* **2012**, *116*, 9379−9389.
(40) Zhang, L.; Cole, J. M. Dye Aggregation in Dye-Sensitized Solar Cells. *J. Mater. Chem. A* **2017**, *5*, 19541−19559.
(41) He, J.; Jo, Y. J.; Sun, X.; Qiao, W.; Ok, J.; Kim, T.-i.; Li, Z. Squaraine Dyes for Photovoltaic and Biomedical Applications. *Adv. Funct. Mater.* **2021**, *31*, 2008201.
(42) Ajayaghosh, A. Chemistry of Squaraine-Derived Materials: Near-IR Dyes, Low Band Gap Systems, and Cation Sensors. *Acc. Chem. Res.* **2005**, *38*, 449−459.
(43) Singh, A. K.; Veetil, A. N.; Nithyanandhan, J. D-A-D Based Complementary Unsymmetrical Squaraine Dyes for Co-Sensitized Solar Cells: Enhanced Photocurrent Generation and Suppressed Charge Recombination Processes by Controlled Aggregation. *ACS Appl. Energy Mater.* **2021**, *4*, 3182−3193.
(44) Alagumalai, A.; Munavvar, M. F.; Vellimalai, P.; Sil, M. C.; Nithyanandhan, J. Effect of Out-of-Plane Alkyl Group's Position in Dye-Sensitized Solar Cell Efficiency: A Structure-Property Relationship Utilizing Indoline-Based Unsymmetrical Squaraine Dyes. *ACS Appl. Mater. Interfaces* **2016**, *8*, 35353−35367.
(45) Singh, A. K.; Maibam, A.; Javaregowda, B. H.; Bisht, R.; Kudlu, A.; Krishnamurty, S.; Krishnamoorthy, K.; Nithyanandhan, J. Unsymmetrical Squaraine Dyes for Dye-Sensitized Solar Cells: Position of the Anchoring Group Controls the Orientation and Self-Assembly of Sensitizers on the TiO_2 Surface and Modulates Its Flat Band Potential. *J. Phys. Chem. C* **2020**, *124*, 18436−18451.
(46) Singh, A. K.; Kavungathodi, M. F. M.; Mozer, A. J.; Krishnamoorthy, K.; Nithyanandhan, J. Solvent-Dependent Functional Aggregates of Unsymmetrical Squaraine Dyes on TiO_2 Surface for Dye-Sensitized Solar Cells. *Langmuir* **2022**, *38*, 14808−14818.
(47) Singh, A. K.; Sudhakar, V.; Javaregowda, B. H.; Bisht, R.; Krishnamoorthy, K.; Nithyanandhan, J. Modular TiO_2-Squaraine

https://doi.org/10.1021/acsomega.4c00123
ACS Omega 2024, 9, 16429−16442

Dyes/Electrolyte Interface for Dye-Sensitized Solar Cells with Cobalt Electrolyte. *ChemPhotoChem* **2022**, *7*, No. e202200171.
(48) Bisht, R.; Mele Kavungathodi, M. F.; Nithyanandhan, J. Indenoquinaldine-Based Unsymmetrical Squaraine Dyes for Near-Infrared Absorption: Investigating the Steric and Electronic Effects in Dye-Sensitized Solar Cells. *Chem.—Eur. J.* **2018**, *24*, 16368−16378.
(49) Zeng, K.; Lu, Y.; Tang, W.; Zhao, S.; Liu, Q.; Zhu, W.; Tian, He.; Xie, Y. Efficient Solar Cells Sensitized by a Promising New type of Porphyrin; Dye-aggregation Suppressed by Double Strapping. *Chem. Sci.* **2019**, *10*, 2186−2192.
(50) Frisch, M. J.; Trucks, G. W.; Schlegel, H. B.; Scuseria, G. E.; Robb, M. A.; Cheeseman, J. R.; Scalmani, G.; Barone, V.; Mennucci, B.; Petersson, G. A.; Nakatsuji, H.; Caricato, M.; Li, X.; Hratchian, H. P.; Izmaylov, A. F.; Bloino, J.; Zheng, G.; Sonneneberg, J. L.; Hada, M.; Ehara, M.; Toyota, K.; Fukuda, R.; Hasegawa, J.; Ishida, M.; Nakajima, T.; Honda, Y.; Kitao, O.; Nakai, H.; Vreven, T.; Montgomery, J. A., Jr.; Peralte, J. E.; Ogliaro, F.; Bearpark, M.; Heyd, J. J.; Brothers, E.; Kudin, K. N.; Staroverov, V. N.; Kobayashi, R.; Normand, J.; Raghavachari, K.; Rendell, A.; Burant, J. C.; Iyenger, S. S.; Tomasi, J.; Cossi, M.; Rega, N., Millam, J. M.; Klene, M.; Knox, J. E.; cross, J. B.; Bakken, V.; Adamo, C.; Jaramillo, J.; Gomperts, R.; Stratmann, R. E.; Yazyev, O.; Austin, A. J.; Cammi, R.; Pomelli, C.; Ochterski, J. W.; Martin, R. L.; Morokuma, K.; Zakrzewski, V. G.; Voth, G. A.; Salvador, P.; Dannenberg, J. J.; Dapprich, S.; Daniels, A. D.; Farkas, O.; Foresman, J. B.; Ortiz, J. V.; Cioslowski, J.; Fox, D. J. *Gaussian 09*, revision A.02; Gaussian, Inc.: Wallingford, CT, 2009.
(51) Kim, B. G.; Chung, K.; Kim, J. Molecular Design principle of All-organic Dyes for Dye-Sensitized Solar Cells. *Chem.—Eur. J.* **2013**, *19*, 5220−5230.
(52) Zhang, F.; Gratzel, M.; Meng, S. Structure-Property Relation in All-organic Dye-Sensitized Solar Cells. *Adv. Funct. Mater.* **2013**, *23*, 424−429.
(53) Wang, Q.; Moser, J. E.; Gratzel, M. Electrochemical Impedance Spectroscopic Analysis of Dye-Sensitized Solar Cells. *J. Phys. Chem. B* **2005**, *109*, 14945−14953.
(54) Bisht, R.; Mele Kavungathodi, M. F.; Singh, A. K.; Nithyanandhan, J. Panchromatic Sensitizer for Dye-Sensitized Solar Cells: Unsymmetrical Squaraine Dyes Incorporating Benzodithiophene π-Spacer with Alkyl Chains to Extend Conjugation, Control the Dye Assembly on TiO_2, and Retard Charge Recombination. *J. Org. Chem.* **2017**, *82*, 1920−1930.

https://doi.org/10.1021/acsomega.4c00123
ACS Omega 2024, 9, 16429−16442